JACS
JOURNAL OF THE AMERICAN CHEMICAL SOCIETY
Article
pubs.acs.org/JACS

Design Strategy for a Near-Infrared Fluorescence Probe for Matrix Metalloproteinase Utilizing Highly Cell Permeable Boron Dipyrromethene

Takuya Myochin, Kenjiro Hanaoka, Toru Komatsu, Takuya Terai, and Tetsuo Nagano*

Graduate School of Pharmaceutical Sciences, The University of Tokyo, 7-3-1 Hongo, Bunkyo-ku, Tokyo 113-0033, Japan

Supporting Information

ABSTRACT: Near-infrared (NIR) fluorescence probes are especially useful for simple and noninvasive *in vivo* imaging inside the body because of low autofluorescence and high tissue transparency in the NIR region compared with other wavelength regions. However, existing NIR fluorescence probes for matrix metalloproteinases (MMPs), which are tumor, atherosclerosis, and inflammation markers, have various disadvantages, especially as regards sensitivity. Here, we report a novel design strategy to obtain a NIR fluorescence probe that is rapidly internalized by free diffusion and well retained intracellularly after activation by extracellular MMPs. We designed and synthesized four candidate probes, each consisting of a cell permeable or nonpermeable NIR fluorescent dye as a Förster resonance energy transfer (FRET) donor linked to the NIR dark quencher BHQ-3 as a FRET acceptor via a MMP substrate peptide. We applied these probes for detection of the MMP activity of cultured HT-1080 cells, which express MMP2 and MT1-MMP, by fluorescence microscopy. Among them, the probe incorporating BODIPY650/665, **BODIPY-MMP**, clearly visualized the MMP activity as an increment of fluorescence inside the cells. We then applied this probe to a mouse xenograft tumor model prepared with HT-1080 cells. Following intratumoral injection of the probe, MMP activity could be visualized for much longer with **BODIPY-MMP** than with the probe containing SulfoCy5, which is cell impermeable and consequently readily washed out of the tissue. This simple design strategy should be applicable to develop a range of sensitive, rapidly responsive NIR fluorescence probes not only for MMP activity, but also for other proteases.

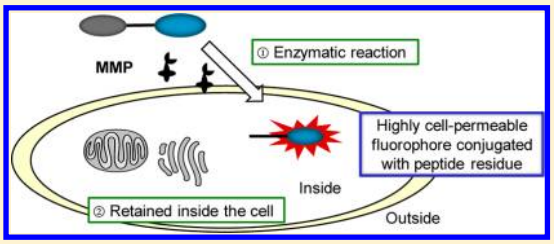

INTRODUCTION

Proteases are involved in the regulation of diverse disease processes and are considered to have potential clinical value both as biomarkers and therapeutic targets. Among them, matrix metalloproteinases (MMPs) are a family of zinc metalloproteinases, which play important roles in degrading the extracellular matrix (ECM) and in both physiological and pathological processes of tissue remodeling.[1] MMPs activity is also considered to be a marker for embryogenesis, wound healing, inflammation, arthritis, cardiovascular disease, and cancer.[2] For example, MMP2 and membrane-type 1 MMP (MT1-MMP) are related to tumor invasion, metastasis, and angiogenesis, and molecular imaging of their activity may be helpful to predict the malignancy of tumors.[3]

Near-infrared (NIR) light, in the wavelength range of 650–900 nm, is especially suitable for noninvasive in vivo imaging,[4] because it is relatively poorly absorbed by biomolecules, so that it can penetrate well through tissues, and background autofluorescence is low in the NIR region.[5] Several NIR fluorescence probes for visualizing MMP activity in vivo have been reported over the past decade. For example, MMPsense680 was used to visualize MMP activity in tumor tissue[6] or atherosclerosis.[7] However, all of these probes suffer from various disadvantages. For example, most MMP probes consist of a fluorophore containing sulfo groups, so the activated probe after the enzymatic reaction with extracellular MMP is highly water soluble and cell impermeable.[8] Consequently, the activated probes are rapidly washed out from the tissue. To overcome this problem, Tsien et al. developed a probe utilizing a cell-penetrating peptide,[9] which enables the MMP-activated probe to penetrate into cells, where it is retained for a relatively long period. However, this probe suffers from toxicity of the cell-penetrating peptide and slow uptake into cells,[10] which occurs via endocytosis or macropinocytosis.[11] Herein, we propose a simple design approach to obtain a highly sensitive fluorescence probe for MMP by utilizing NIR fluorescent dyes that exhibit high cell permeability via rapid free diffusion and good intracellular retention after activation (Figure 1), thereby providing a well-sustained fluorescence signal with very high signal-to-noise ratio.

RESULTS AND DISCUSSION

Design and Synthesis of NIR Fluorescence Probes for MMP Activity. We employed Förster resonance energy transfer (FRET) as a fluorescence-controlling off/on mechanism. Specifically, we conjugated a fluorophore as a FRET donor and a dark nonfluorescent quencher as a FRET acceptor to the opposite terminals of a MMP peptide substrate. This

Received: April 24, 2012
Published: July 25, 2012

dx.doi.org/10.1021/ja303931b | J. Am. Chem. Soc. 2012, 134, 13730–13737

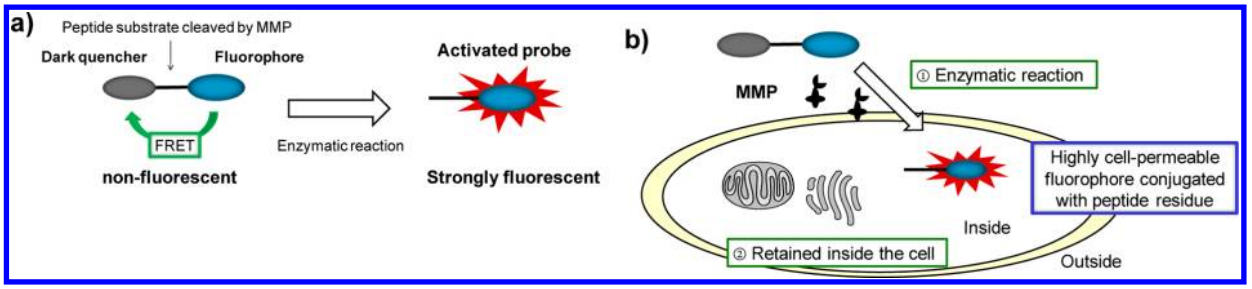

Figure 1. (a) Design of our activatable MMP probe based on the FRET mechanism. (b) The strategy used to achieve long-term retention of the MMP probe in the tissue after enzymatic reaction. The activated probe is cell permeable. Intracellular retention is dependent on the chemical structure of the activated probe, i.e., the cell permeable fluorophore conjugated with the peptide residue.

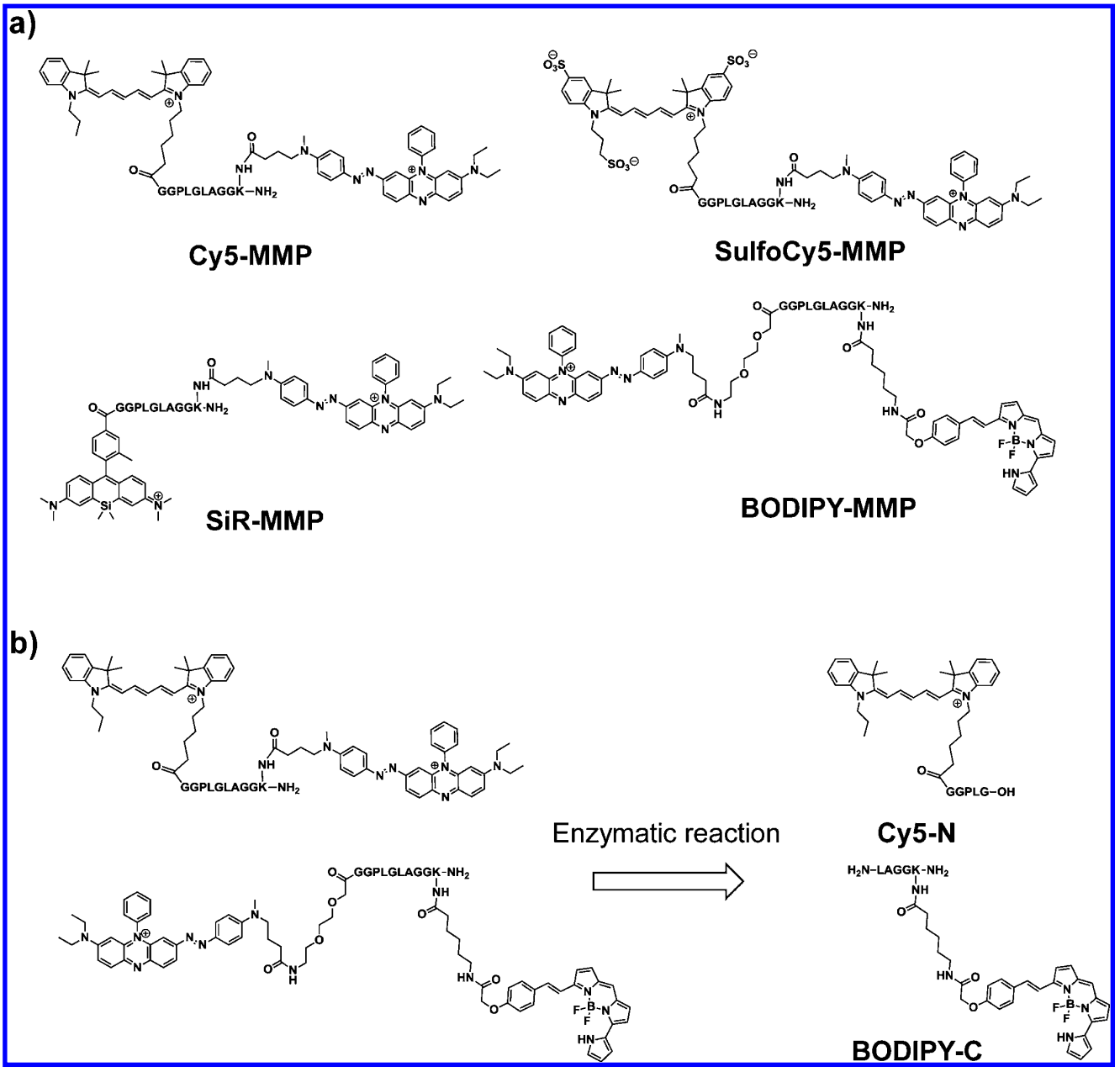

Figure 2. (a) Chemical structures of MMP probes with the four NIR fluorophores. (b) Chemical structures of the expected MMP-generated cleavage products of **Cy5-MMP** and **BODIPY-MMP**, i.e., **Cy5-N** and **BODIPY-C**, respectively.

FRET strategy is often used in fluorescence probes to detect protease activity, because a very high signal-to-noise ratio can easily be achieved, i.e., the fluorescence intensity of the fluorophore is strongly suppressed before the enzymatic reaction.[12] In this study, we used BHQ-3 as the dark quencher, together with four NIR fluorophores (Cy5, BODIPY650/665,

dx.doi.org/10.1021/ja303931b | J. Am. Chem. Soc. 2012, 134, 13730–13737

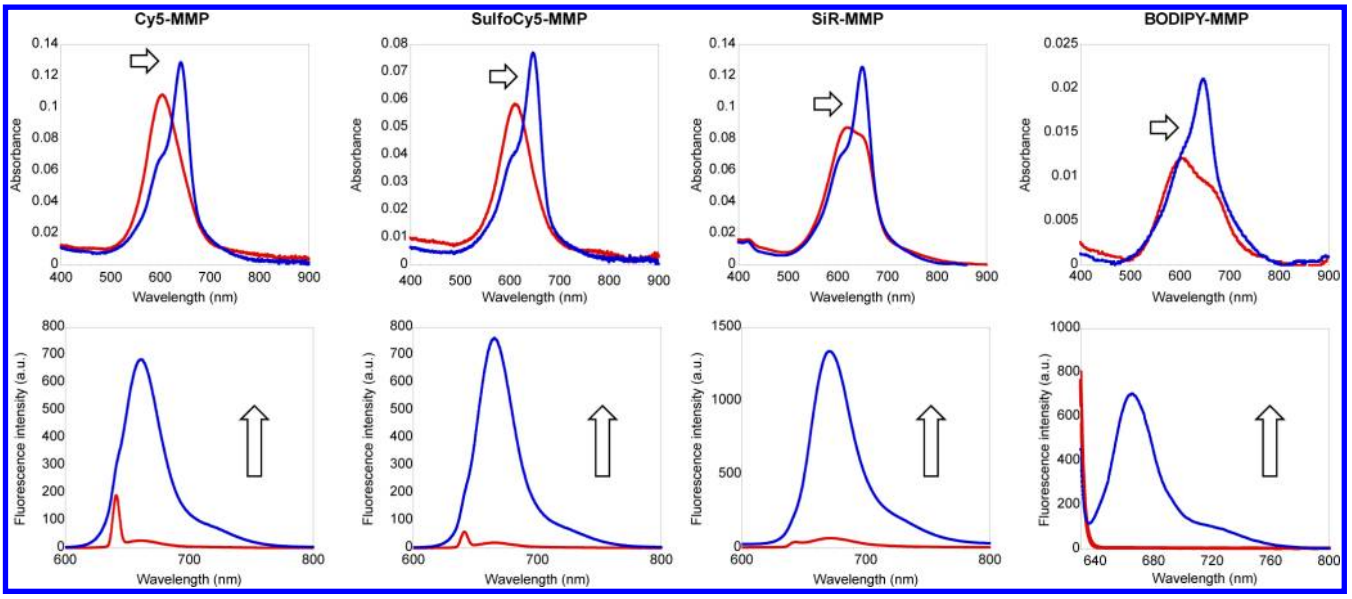

Figure 3. (Top) Absorption spectra before (red) and after enzymatic reaction (blue) of the four MMP probes, **Cy5-MMP** (1 μM), **SulfoCy5-MMP** (1 μM), **SiR-MMP** (1 μM), **BODIPY-MMP** (2 μM) in 1 mL TCN buffer containing 0.1% DMSO (for **Cy5-MMP**, **SulfoCy5-MMP**, and **SiR-MMP**) or 3% DMSO (for **BODIPY-MMP**) as a cosolvent. (bottom) Fluorescence spectra of the MMP probes, **Cy5-MMP** (1 μM), **SulfoCy5-MMP** (1 μM), **SiR-MMP** (1 μM), **BODIPY-MMP** (2 μM), incubated with 1 μg of MMP2 (catalytic domain recombinant protein) in 1 mL TCN buffer containing 0.1% DMSO (for **Cy5-MMP**, **SulfoCy5-MMP**, and **SiR-MMP**) or 3% DMSO (for **BODIPY-MMP**) as a cosolvent at 37 °C for 300 min (**Cy5-MMP**), 840 min (**SulfoCy5-MMP**), 600 min (**SiR-MMP**), or 240 min (**BODIPY-MMP**) with excitation at 620 nm (for **BODIPY-MMP**) or 640 nm (for **Cy5-MMP**, **SulfoCy5-MMP**, and **SiR-MMP**). Spectra were measured before (red) and after (blue) enzymatic reaction.

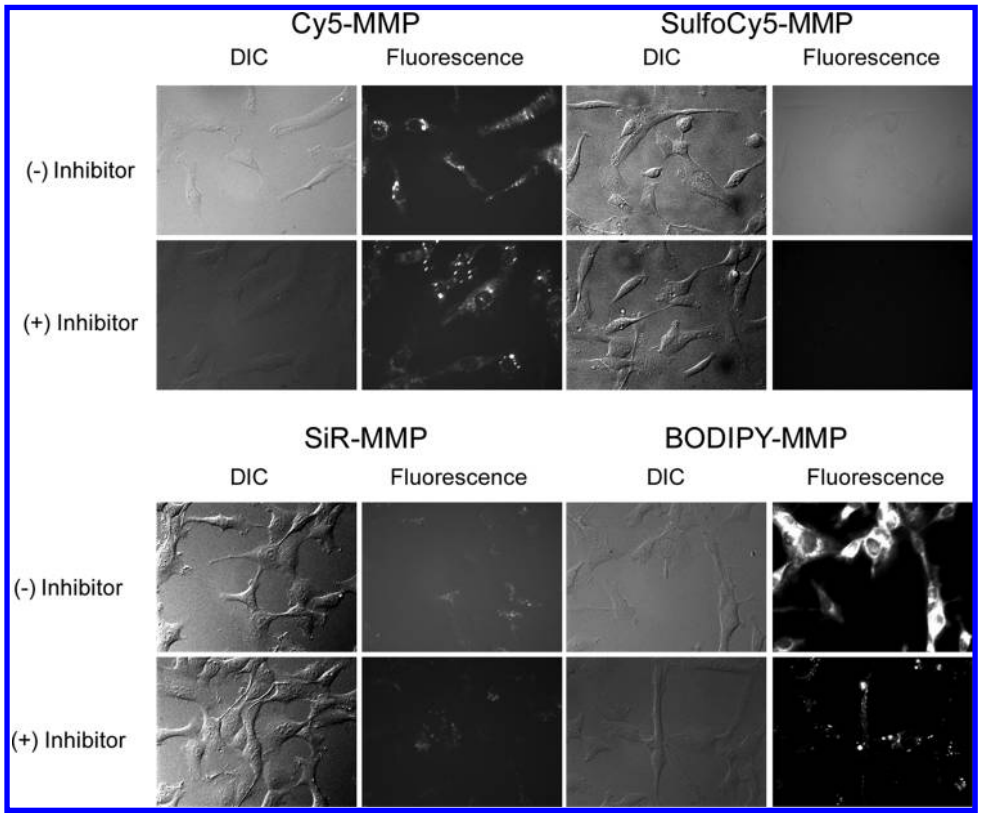

Figure 4. Bright field and fluorescence images of HT-1080 cells incubated with **Cy5-MMP**, **SulfoCy5-MMP**, **SiR-MMP**, or **BODIPY-MMP** (1 μM, final 0.2% DMSO as a cosolvent) at 37 °C for 3 h in the presence (bottom) or the absence (top) of the inhibitor GM6001 (100 μM).

SiR650, and SulfoCy5) and a MMP substrate peptide as a linker moiety (Figure 2a). Cy5 is one of the cyanine dyes, which are typical NIR fluorophores.[13] BODIPY650/665 is based on a BODIPY (boron dipyrromethene) scaffold with a relatively sharp NIR fluorescence peak and high quantum yield. BODIPY dyes are relatively insensitive to the polarity and pH of their environment.[14] SiR650 is a novel NIR fluorophore which is more resistant to bleaching than other NIR

dx.doi.org/10.1021/ja303931b | J. Am. Chem. Soc. 2012, 134, 13730−13737

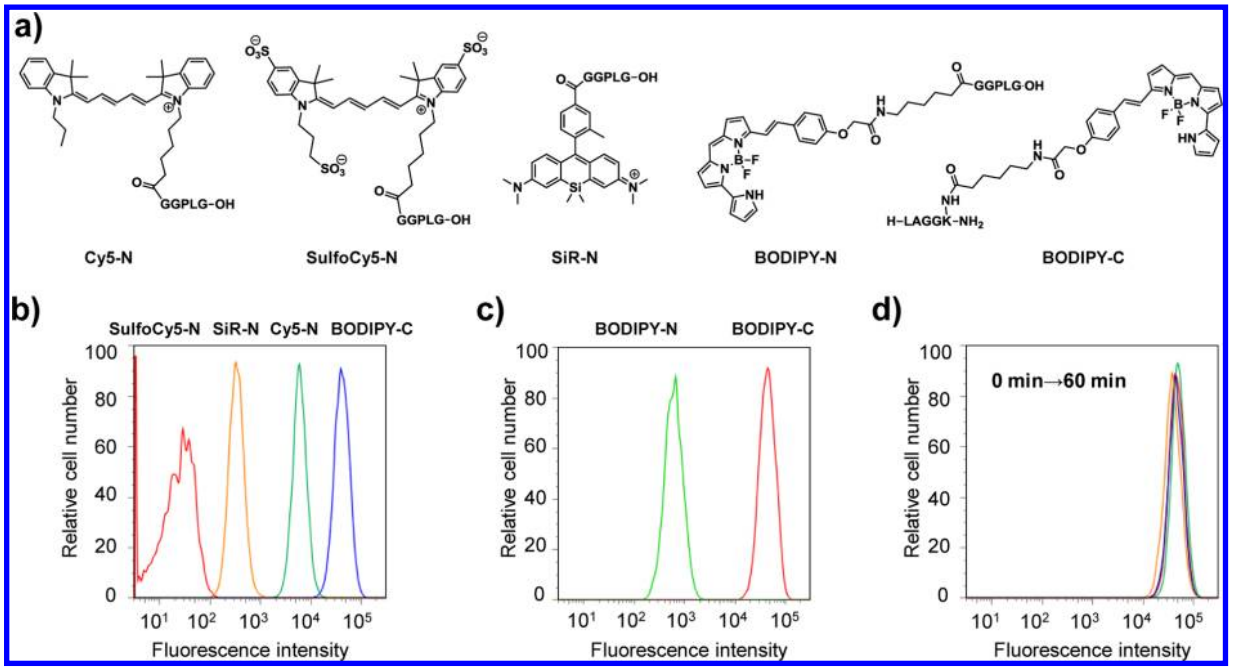

Figure 5. (a) Chemical structures of additionally synthesized compounds: peptide residues conjugated with various NIR fluorophores. (b) Flow cytometric analysis of HT-1080 cells loaded with **SulfoCy5-N** (red), **SiR-N** (orange), **Cy5-N** (green), or **BODIPY-C** (blue). Each probe was used at a final concentration of 1 μM in HBSS containing 0.1% DMSO as a cosolvent, and cells were incubated for 1 h at 37 °C. (c) Flow cytometric analysis of HT-1080 cells incubated with **BODIPY-N** (green) or **BODIPY-C** (red) (final 1 μM, 0.1% DMSO as a cosolvent) at 37 °C. (d) Flow cytometric analysis of HT-1080 cells incubated with **BODIPY-C** (final 1 μM, 0.1% DMSO as a cosolvent) for 1 h at 37 °C, washed with PBS, and then incubated with HBSS for 0 min (green), 15 min (red), 30 min (blue), and 60 min (orange).

fluorophores.[15] SulfoCy5, which has three sulfo groups, is also a typical cyanine dye, and is cell impermeable due to its anionic charges. Cy5, BODIPY650/665, and SiR650 are highly cell permeable, and thus we anticipated that activated fluorescence probes based on them would become cell permeable after MMP enzymatic reaction. On the other hand, the MMP fluorescence probe containing SulfoCy5 may be cell impermeable both before and after the MMP enzymatic reaction. We synthesized **SulfoCy5-MMP** to assess the effect of the cell permeability of the fluorophore on fluorescence imaging of MMP activity in cultured live cells. The peptide linking the fluorophore and dark quencher contains a PLGLAG peptide sequence, which is selectively cleaved by MMP2, MMP9, and MT1-MMP.[16] Thus, we designed and synthesized four candidate NIR fluorescence probes for MMP activity with the four NIR fluorophores; the peptide linker was obtained by Fmoc solid-phase peptide synthesis. We initially tried to conjugate the fluorophore to the N-terminal and BHQ-3 to the C-terminal of the peptide substrate, and successfully synthesized **Cy5-MMP**, **SulfoCy5-MMP**, and **SiR-MMP**. However, it proved difficult to synthesize the probe with BODIPY650/665 conjugated to the N-terminal of the peptide. So, only in the case of BODIPY650/665, we designed and synthesized the probe with the fluorophore at the C-terminal of the peptide substrate (Figure 2b and Supporting Information [SI]).

Fluorescence and Chemical Properties of the MMP Probes. We examined the spectroscopic properties of the four synthesized MMP probes under physiological conditions. The absorption spectra of the probes changed after addition of MMP2 or MT1-MMP in accordance with the change in fluorescence emission spectra (Figure 3, and Figures S1−S4 [SI]), i.e., before addition of MMP, the fluorescence intensity of each probe was negligible, and a blue-shift of the absorption was observed compared with the spectrum of the fluorophore alone. This blue-shift of the absorption is considered to be due to stacking interaction between the fluorophore and BHQ-3. The fluorescence quantum yields of all the probes were less 0.001 owing to FRET and the stacking interaction.[17] After addition of MMP, the absorption spectrum of each probe corresponded to the combined spectrum of the fluorophore and BHQ-3, and the fluorescence intensities of all the MMP probes also increased. The kinetic parameter of these probes with MMP2, V_{max}/K_m, was determined by applying the equation shown in Table S1 (SI). As compared with the commercially available Omni fluorescence substrate, which is often used to detect MMP activity *in vitro*, all the probes seemed to be cleaved rapidly by MMP. HPLC analysis confirmed that all the probes were cleaved by MMP2, as expected (Figure S5−S8 [SI]).

Live Cell Fluorescence Imaging of MMP Activity. We applied the four probes to cultured HT-1080 cells, which express MMP2 and MT1-MMP,[18] to assess their intracellular retention after enzymatic reaction by means of fluorescence microscopy. The cells were incubated with 1 μM MMP probe for 180 min in the absence or presence of 100 μM GM6001, which is a broad-spectrum MMP inhibitor. **BODIPY-MMP** showed a large increase of intracellular fluorescence in the absence of GM6001, and this fluorescence increment was suppressed in the presence of GM6001 (Figure 4). On the other hand, no significant difference of intracellular fluorescence was observed between the absence and presence of GM6001 with the other probes, i.e., essentially no fluorescence increment inside cells was observed, even though the extracellular fluorescence intensity was increased (Figure 4). From these results, it is considered that all the probes were cleaved by MMPs, but **Cy5-MMP**, **SulfoCy5-MMP**, and **SiR-**

dx.doi.org/10.1021/ja303931b | J. Am. Chem. Soc. 2012, 134, 13730−13737

MMP remained in the extracellular environment after the enzymatic reaction. On the other hand, MMP-activated **BODIPY-MMP** penetrated into the cells and afforded clear cellular images. We further confirmed the high intracellular retention of **BODIPY-MMP** by flow cytometric analysis (see Figure S9, SI). It is difficult to completely rule out the possibility that a part of the MMP probe enters the cells intact and is cleaved by intracellular MMPs, such as MT1-MMP. However, we think that most of the **BODIPY-MMP** molecules were cleaved by extracellular MMP, as planned, because the increase of fluorescence intensity inside the cultured cells was suppressed by adding to the medium ethylenediaminetetraacetic acid (EDTA), which is cell impermeable and inhibits only extracellular MMP activity (Figure S10, SI).[19]

Detailed Investigation of the Cell Permeability of MMP Probes after Enzymatic Reaction with MMP. Next, to further examine the cell permeability of **BODIPY-MMP** after enzymatic reaction with MMP, we synthesized **Cy5-N**, **SulfoCy5-N**, **SiR-N**, and **BODIPY-C**, corresponding to the structures of the four probes after enzymatic reaction with MMP, i.e., the fluorophores conjugated with the peptide residue (Figure 5a). The fluorescence quantum yields of these molecules were over 0.1 (Table 1). Cultured HT-1080 cells were incubated with each probe (1 μM) for 60 min and analyzed by flow cytometry. **BODIPY-C** gave the highest intracellular fluorescence intensity among the four compounds (Figure 5b). But, flow cytometric analysis is often influenced by the inherent photophysical properties of fluorescent dyes, i.e., both the extinction coefficient and the fluorescence quantum yield of the fluorophore. So, we next conducted fluorescence imaging of HT-1080 cells incubated with the four synthesized molecules by means of fluorescence microscopy with or without a washout process (Figure S11, SI). Only **BODIPY-C** clearly stained the cells both before and after washout of the extracellular solution. On the other hand, **Cy5-N**, **SiR-N**, and **SulfoCy5-N** poorly stained the cells, and the extracellular solution showed intense fluorescence intensity. These results indicate that **BODIPY-C** is highly cell permeable, whereas the other compounds are insufficiently permeable to image the cells clearly. These results are consistent with those of fluorescence imaging with the MMP probes (Figure 4).

Table 1. Fluorescence Quantum Yields of the MMP Probes.[a]

	Cy5	SulfoCy5	SiR	BODIPY
MMP probes	<0.001	<0.001	<0.001	<0.001
synthetic cleaved MMP probe	0.129	0.179	0.169	0.127

[a]Fluorescence quantum yields were determined in TCN buffer (pH 7.4), referring to that of cresyl violet (Φ_{fl} = 0.54) in methanol as a standard.

We further investigated the effect of the fluorophore-conjugated terminal, i.e., the N-terminal or the C-terminal of the peptide substrate, on the cell permeability of the activated MMP probes. Compounds with N-terminal BODIPY650/665 (**BODIPY-N**) and C-terminal Cy5 (**Cy5-C**) (Figure S12, SI) were further synthesized. Flow cytometric analysis indicated that the C-terminal dye was more cell permeable than the N-terminal dye for both BODIPY650/665 and Cy5 as a fluorophore (Figures 5c and S12, SI). Thus, the cell permeability of the MMP probe after enzymatic reaction appears to depend on both the fluorophore and the conjugated peptide. The effect of the fluorophore may be based on both its lipophilicity and electric charge, while the effect of the peptide residue may depend upon both the nature of the side chains and the peptide terminal generated by MMP, i.e., carboxylic acid or amino group.

We also examined the intracellular retention of **BODIPY-C** in HT-1080 cells by means of flow cytometry. The intracellular fluorescence of **BODIPY-C** was still intense even at 60 min after excess probe had been washed out with phosphate-buffered saline (PBS) (Figure 5d). The fluorescence intensity of stained cells remained almost unchanged during incubation for 0 to 60 min in PBS after washout of the extracellular solution. We also examined the localization of **BODIPY-C** inside cells, and found that fluorescence of **BODIPY-C** was observed mainly in mitochondria and Golgi bodies (Figure S13, SI). We think that this intracellular localization contributes to the efficient long-term intracellular retention.

***In Vivo* Imaging in Tumor-Bearing Mouse.** Finally, we applied **BODIPY-MMP** to visualize the MMP activity of tumor tissue *in vivo*. **BODIPY-MMP** was injected intratumorally into a HT-1080 tumor-bearing mouse, and the change in the fluorescence intensity was monitored (Figure 6). The fluorescence of **BODIPY-MMP** was clearly detected at the tumor after 15 min and was well maintained for over 6 h, while the fluorescence of the **SulfoCy5-MMP**, of which the activated form is cell impermeable, was detected at both the tumor and throughout the whole body soon after the intratumoral injection, presumably due to rapid diffusion of the dye over the body, but the tumor was no longer detectable after 60 min. To confirm that the activated probe after administration of **BODIPY-MMP** was indeed present intracellularly in vivo, the tumor at 360 min after intratumoral injection of **BODIPY-MMP** was removed and imaged by confocal fluorescence microscopy at the cellular level (Figure S14, SI). The fluorescence of **BODIPY-MMP** was indeed detected inside cells of the tumor tissue, as in the case of the experiments with cultured HT-1080 cells. So, it is considered that **BODIPY-MMP** was also cleaved by MMP in the tumor tissue and the activated **BODIPY-MMP**, i.e., **BODIPY-C**, was introduced into cells *in vivo*. We further assessed whether the increment of the fluorescence intensity of **BODIPY-MMP** *in vivo* was due to MMP enzymatic activity. To address this question, we newly synthesized **ControlBODIPY-MMP**, which has the reverse peptide sequence of the peptide substrate for MMP2, MMP9 and MT1-MMP, and is not cleaved by MMP.[16] When we intratumorally injected **ControlBODIPY-MMP** into the tumor, only a minor fluorescence enhancement, which might be due to the relative instability of BHQ-3,[20] was observed compared with the case of **BODIPY-MMP** injection (Figure 6). Therefore, we consider that the difference of the fluorescence enhancement of **BODIPY-MMP** and **ControlBODIPY-MMP** reflected the MMP activity *in vivo*.

Next, to examine whether the long-term retention in the tumor tissue was related to the cell permeability of **BODIPY-C** or **SulfoCy5-N**, we intratumorally injected these compounds, which are the products of the enzymatic reaction of **BODIPY-MMP** or **SulfoCy5-MMP** with MMP, respectively, and the time course of fluorescence intensity change at the tumor was monitored (Figure 6c). Although the fluorescence of **SulfoCy5-N**, which is cell impermeable, was quickly washed out from the tumor tissue and disappeared from the whole body after 30 min, the fluorescence of **BODIPY-C**, which has high cell permeability, was highly retained in the tumor even after 6 h (data not shown). These results suggest that high cell

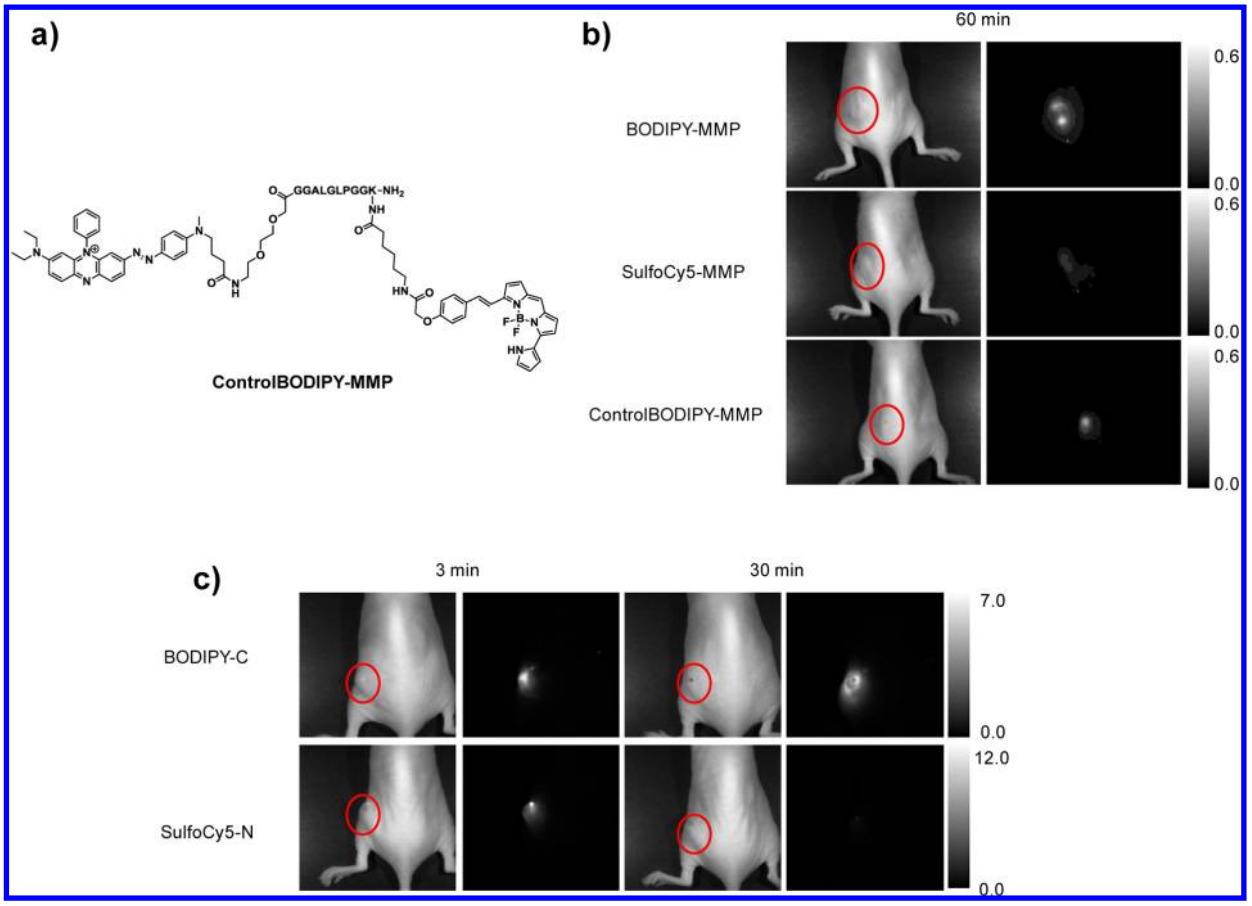

Figure 6. (a) Chemical structure of **ControlBODIPY-MMP**. (b) White light (left) and fluorescence (right) images of HT-1080 tumor-bearing nude mouse at 60 min after the injection. **BODIPY-MMP** (top), **SulfoCy5-MMP** (middle) or **ControlBODIPY-MMP** (bottom) (10 μM in 20 μL PBS containing 1% DMSO as a cosolvent) was administrated by intratumoral injection. Images were captured at 120 min after the injection. The site of the tumor is indicated by red circles. (c) White light and fluorescence images of HT-1080 tumor-bearing nude mouse at 3 and 30 min after the injection. **BODIPY-C** (top) or **SulfoCy5-N** (bottom) (1 μM in 20 μL PBS containing 0.1% DMSO as a cosolvent) was administered by intratumoral injection.

permeability of the activated MMP probe after enzymatic reaction is critical for long-term dye retention in the target tissue and for in vivo fluorescence imaging with a high signal-to-noise ratio.

CONCLUSIONS

In conclusion, we have designed, synthesized, and evaluated a novel MMP probe, **BODIPY-MMP**. Our design approach was to conjugate a fluorophore as a FRET donor and a dark quencher as a FRET acceptor at the opposite ends of a MMP peptide substrate. To achieve long-term retention of the probe at the target site and a high signal-to noise ratio, we focused on high cell permeability of the MMP-activated probe, which was consequently expected to be accumulated intracellularly at the target tissue following the extracellular MMP reaction, instead of being washed out, as is the case for cell impermeable activated probes. **BODIPY-MMP** could clearly visualize MMP activity as a fluorescence increment inside cultured HT-1080 cells. Further, following intratumoral injection of **BODIPY-MMP** in a mouse xenograft tumor model, the MMP activity could be monitored (i.e., the tumor could be visualized) for much longer than the case with the probe containing cell impermeable SulfoCy5. In contrast to previously reported probes, this probe offers the advantages of rapid and sustained response with a high signal-to-noise ratio. We think this simple design strategy will be applicable to a range of NIR fluorescence probes, not only for MMP activity, but also other proteases.

EXPERIMENTAL SECTION

Reagents and solvents were of the best grade available, supplied by Tokyo Chemical Industries, Wako Pure Chemical, Aldrich Chemical Co., Biosearch Technology, Kanto Chemical Company, Watanabe Chemical Industry, Applied Bioscience or Invitrogen, and were used without further purification. Saline was purchased from Otsuka Pharmaceutical Co. Ltd. Mice (BALB/cAJcl-nu/nu) were purchased from CLEA Japan. Reactions were monitored by TLC with visual observation of the dye spot or by HPLC. All compounds were purified on a silica gel column and by HPLC. All fluorescent probes were considered pure when a single HPLC peak was obtained.

Instruments. ^{1}H or ^{13}C NMR spectra were recorded on a JEOL JNM-LA300 or JMN-LA400. Mass spectra were measured with a JEOL JMS-T1000LC mass spectrometer (ESI^{+} and ESI^{-}). HPLC purification and analyses were performed on reversed-phase columns (GL Science (Tokyo, Japan), Inertsil ODS-3 10 mm ×250 mm for purification and Inertsil ODS-3 4.6 mm ×250 mm for analyses) fitted on a Jasco PU-2080 system and eluted with eluent A (H_2O containing 0.1% TFA (v/v)) and eluent B (CH_3CN with 20% H_2O containing 0.1% TFA (v/v)). Details of HPLC conditions are included with the synthesis and characterization data. Absorption spectra were obtained with a Shimadzu UV-1650 (Tokyo, Japan). Fluorescence spectroscopic studies were performed with a Hitachi F4500 (Tokyo, Japan). The slit widths were 2.5 nm for excitation and 5 nm for emission. The photomultiplier voltage was 700 V. Peptide synthesis was performed

dx.doi.org/10.1021/ja303931b | J. Am. Chem. Soc. 2012, 134, 13730−13737

with 433A peptide Synthesizer (Applied Biosystems, U.S.A.) and SynthAssist 3.1 (Applied Biosystems, U.S.A.).

Photochemical Properties and Fluorescence Quantum Yield. Photochemical properties of dyes were examined in TCN buffer (50 mM Tris, 10 mM $CaCl_2$, 150 mM NaCl) (pH 7.5) containing 0.1% DMSO as a cosolvent, using a Shimadzu UV-1650 UV−vis spectrometer and a Hitachi F4500 fluorescence spectrometer. For determination of the fluorescence quantum yield (Φ_{fl}), cresyl violet in methanol (Φ_{fl} = 0.54) was used as a standard, and the results were calculated according to the following equation (subscript "st" stands for the reference, and "x", for the sample).

$$\Phi_x/\Phi_{st} = [A_{st}/A_x][n_x^2/n_{st}^2][D_x/D_{st}]$$

where A = absorbance at the excitation wavelength; n = refractive index; and D = area under the fluorescence spectra on an energy scale.

Enzyme Assay. One microgram MMP2 catalytic domain (human) (ENZO Life Science, U.S.A.) in 2 μL TCNB buffer (50 mM Tris, 10 mM $CaCl_2$, 150 mM NaCl, 0.05% Brij 35) (pH 7.5) or 1 μg MT1-MMP catalytic domain (human) (Calbiochem, U.S.A.) in 2 μL TCNB buffer was incubated for 15 min at 37 °C before the enzyme assay. Each probe was used at a final concentration of 1 or 2 μM in 1 mL TCN buffer containing 0.1% (**Cy5-MMP**, **SulfoCy5-MMP**, **SiR-MMP**) or 3% (**BODIPY-MMP**) DMSO as a cosolvent at 37 °C. Fluorescence spectra were measured every 10 min after the enzyme solution was added until termination of the enzymatic reaction.

HPLC Analysis. Ten micromolar synthesized MMP probe was dissolved in 1 mL TCN buffer containing 1% DMSO as a cosolvent, and 1 μg MMP2 catalytic domain (ENZO Life Science) was added to the solution, which was then incubated at 37 °C for 6 h. The solution was lyophilized, and 30 μL DMF/30 μL TCN buffer was added to the residue. This solution was analyzed by HPLC. HPLC analysis: eluent, a 20- or 40-min linear gradient from 20% to 100% solvent B; flow rate, 1.0 mL/min; detection wavelength, 640 nm.

Determination of Kinetic Parameters. Synthesized MMP probe (0.1 μM) was dissolved in 3 mL TCN buffer containing 0.1% DMSO as a cosolvent, and the solution was incubated at 37 °C. One microgram MMP2 (human) (Sigma, U.S.A.) in 20 μL TCNB buffer incubated at 37 °C for 15 min was added to the solution, and the fluorescence intensity change was recorded at 37 °C. The time course of fluorescence intensity was fitted to the equation shown in Table S1 in the Supporting Information to determine V_{max}/K_m.

Cell Lines and Culture Conditions. Human fibrosarcoma cell line HT-1080 was purchased from the Health Science Research Resource Bank (Osaka, Japan). HT-1080 cells were cultured in EMEM (Eagle's minimal essential medium) (Wako), containing nonessential amino acids (Invitrogen), 10% fetal bovine albumin (Invitrogen) and 1% penicillin/streptomycin (Invitrogen). Cultured cells were incubated at 37 °C in an atmosphere of 5% CO_2 in air.

Fluorescence Microscopic Imaging with MMP Probes. HT-1080 cells seeded on an 8-chamber plate (Thermo Scientific, U.S.A.) were washed with PBS, then 200 μL HBSS was added. GM6001 (final 100 μM containing 0.1% DMSO as a cosolvent) was added to the medium in the case of the sample with the inhibitor, while 0.2 μL DMSO was added to the medium in the case of the sample without the inhibitor. The samples were incubated at 37 °C for 15 min. Then, **Cy5-MMP**, **SulfoCy5-MMP**, **SiR-MMP**, or **BODIPY-MMP** (final 1 μM, DMSO 0.2% as a cosolvent) was added to the medium, and incubation was continued at 37 °C. Fluorescence images were captured without washout of excess probe at 3 h after addition of the probe to the medium.

For fluorescence microscopic imaging with **BODIPY-MMP** and EDTA, HT-1080 cells seeded on an 8-chamber plate (Thermo Scientific, U.S.A.) were washed with PBS, then 200 μL HBSS was added. 0.1 M EDTA2Na in 2 μL PBS (final 1 mM) was added to the medium in the case of the sample with the inhibitor, whereas 2 μL PBS was added to the medium in the case of the sample without the inhibitor. The samples were incubated at 37 °C for 15 min. Then, **BODIPY-MMP** (final 1 μM, DMSO 0.1% as a cosolvent) was added to the medium, and incubation was continued at 37 °C. Fluorescence images were captured without washout of excess probe at 15 min after addition of the probe to the medium.

For fluorescence microscopic imaging with the synthesized cleaved probes, HT-1080 cells seeded on an 8-chamber plate (Thermo Scientific, U.S.A.) were washed with PBS, then 200 μL HBSS was added. After that, **Cy5-N**, **SulfoCy5-N**, **SiR-N**, or **BODIPY-C** (final 1 μM, DMSO 0.1% as a cosolvent) was added to the medium, and incubation was continued at 37 °C. Fluorescence images were captured without washout of excess probe at 1 h after addition of the probe to the medium. The HT-1080 cells were washed with PBS, then 200 μL HBSS was added, and fluorescence images were captured with an Olympus IX 71 equipped with a cooled CCD camera (Coolsnap HQ, Olympus) and a xenon lamp (AH2RX-T, Olympus) with a Cy5 excitation filter and a Cy5 emission filter.

Flow Cytometric Analysis. HT-1080 cells plated on a multiwell 12-well plate (Falcon) were washed with PBS, then 1 mL HBSS was added. GM6001 (final 100 μM containing 0.1% DMSO as a cosolvent) was added to the medium in the case of the sample with the inhibitor, whereas 1 μL DMSO was added to the medium in the case of the sample without the inhibitor. The samples were incubated at 37 °C for 15 min. Then, the sample was incubated with synthesized probe (final 1 μM, 0.2% DMSO as a cosolvent) in HBSS at 37 °C for 1 h. The cells were washed with PBS and trypsinized. HBSS was added, and the fluorescence intensity was measured with a BD LSR 2 flow cytometer (BD Biosciences) and FlowJo (Digital Biology). The excitation wavelength was 633 nm, and the emission was detected with an APC filter 660 ± 20 nm.

For examination of the cell permeability of the synthesized cleaved MMP probes, HT-1080 cells on a multiwell 12-well plate (Falcon) were washed with PBS, then 1 mL HBSS was added. Then, the sample was incubated with synthesized cleaved probe (final 1 μM, 0.1% DMSO as a cosolvent) in HBSS at 37 °C for 1 h. The cells were washed with PBS and trypsinized. HBSS was added, and the fluorescence intensity was measured with a BD LSR 2 flow cytometer (BD Biosciences) and FlowJo (Digital Biology).

Analyses of Intracellular Retention of BODIPY-C. HT-1080 cells plated on a multiwell 12-well plate (Falcon) were washed with PBS, then 1 mL HBSS was added. The sample was incubated with **BODIPY-C** (final 1 μM, 0.1% DMSO as a cosolvent) in HBSS at 37 °C for 1 h. Then, the cells were washed with PBS and trypsinized. HBSS was added, and flow cytometric analysis was performed with a BD LSR 2 flow cytometer (BD Biosciences) and FlowJo (Digital Biology). The time course of fluorescence intensity change was measured at 0, 15, 30, and 60 min after addition of HBSS.

Fluorescence Confocal Microscopy. HT-1080 cells seeded on an 8-chamber plate (Thermo Scientific, U.S.) were washed with PBS, then incubated in HBSS containing 0.5 μM NBD C_6-ceramide-BSA at 4 °C for 60 min. The cells were washed with PBS, and incubated in HBSS containing 1 μM **BODIPY-C** and 0.5 μM MitoTracker red containing 0.2% (v/v) DMSO as a cosolvent at 37 °C for 30 min. Fluorescence images were captured using a Leica TCS SP5 confocal microscope equipped with a 40× objective lens using Leica Application Suite Advanced Fluorescence (LAS-AF) software. The light source was a white-light laser. The excitation wavelength was 470 nm (NBDC_6-ceramide-BSA), 579 nm (MitoTracker red), and 640 nm (**BODIPY-C**), and emission wavelength was 492−542 nm (NBDC_6-ceramide-BSA), 592−620 nm (MitoTracker red), and 659−751 nm (**BODIPY-C**). PMT; Gain: 1065 V (NBDC_6-ceramide-BSA), 1000 V (MitoTracker red) and 802 V (**BODIPY-C**), Offset 0%.

Mouse Models. All procedures were approved by the Animal Care and Use Committee of the University of Tokyo. Fluorescence imaging with synthesized MMP probes was performed in BALB/cAJcl-nu/nu mice (6−7 weeks, ♀), each bearing a HT-1080 xenograft tumor prepared by injection of two million cells into the left hind leg at 7−14 days before the probe injection.

***In Vivo* Fluorescence Imaging of Mice after Intratumoral Injection of Fluorescence Probes.** All procedures were approved by the Animal Care and Use Committee of the University of Tokyo. After intratumoral injection of 10 μM **BODIPY-MMP**, **SulfoCy5-MMP**, or **ControlBODIPY-MMP** in 20 μL PBS containing 1%

DMSO as a cosolvent, bright field and fluorescence images were captured at different time points with a Maestro In-vivo Imaging System (CRi Inc., Woburn, MA), with an excitation filter of 635 nm, an emission filter of 675 nm, and bright field settings. All image analyses were performed using Image J (NIH, Bethesda, MD, U.S.A.).

For in vivo imaging of mice with the synthesized cleaved MMP probe, 1 μM **BODIPY-C** or **SulfoCy5-N** in 20 μL PBS containing 0.1% DMSO as a cosolvent, was administered by intratumoral injection, and bright field and fluorescence images were captured at different time points with the same instruments.

Confocal Fluorescence Imaging of Live Mouse Tumor Tissue. All procedures were approved by the Animal Care and Use Committee of the University of Tokyo. Mice were sacrificed and the tumors removed and kept on ice in HBSS until imaging. Each tumor was sliced, placed on a 35 mm glass-bottomed dish, and incubated with Calcein-AM (final 1 μM, 0.1% DMSO as a cosolvent) in HBSS for 30 min, then imaged by confocal microscopy. The excitation wavelengths were 493 nm (Calcein) and 640 nm (**BODIPY-MMP**), and emission wavelengths were 502−562 nm (Calcein) and 659−751 nm (**BODIPY-MMP**), respectively. PMT; Gain: 800 V (Calcein), 550 V (**BODIPY-MMP**), Offset 0%.

■ ASSOCIATED CONTENT

Supporting Information

Detailed descriptions of synthetic procedures for the MMP probes; data on the measurements of absorption and fluorescence spectra of the MMP probes treated with MT1-MMP; HPLC chromatograms of the MMP probes, the reaction mixture of the MMP probes incubated with MMP2, and the synthesized cleaved MMP probes; V_{max}/K_m values of the MMP probes for MMP2; flow cytometric analysis of HT-1080 cells loaded with the MMP probes in the presence or the absence of MMP inhibitor; DIC and fluorescence images of HT-1080 cells stained with **BODIPY-MMP** in the presence or absence of EDTA; fluorescence images of HT-1080 cells incubated with the MMP probe residue; fluorescence images of HT-1080 cells incubated with **BODIPY-C**, $NBDC_6$-ceramide-BSA, and MitoTracker red; bright field and confocal fluorescence images of live mouse tumor tissue loaded with Calcein-AM and **BODIPY-MMP**; white light and fluorescence images of HT-1080 tumor-bearing mouse loaded with **BODIPY-C** or **SulfoCy5-N**. This material is available free of charge via the Internet at http://pubs.acs.org.

■ AUTHOR INFORMATION

Corresponding Author

tlong@mol.f.u-tokyo.ac.jp

Notes

The authors declare no competing financial interest.

■ ACKNOWLEDGMENTS

This research was supported in part by the Ministry of Education, Culture, Sports, Science and Technology of Japan (Specially Promoted Research Grant Nos. 22000006 to T.N. and 20689001, 19890047, 21659024, and 24659042 to K.H.), and SENTAN, JST (to K.H). K.H. was also supported by Grant-in-Aid from the Tokyo Biochemical Research Foundation, Inoue Foundation for Science, Takeda Science Foundation, the Research Foundation for Pharmaceutical Sciences, Konica Minolta Science and Technology Foundation, The Asahi Glass Foundation and Astellas Foundation for Research on Metabolic Disorders.

■ REFERENCES

(1) (a) Seiki, M. *Curr. Opin. Cell. Biol.* **2002**, *14*, 624−632. (b) Seiki, M.; Itoh, Y. *J. Cell. Phys.* **2006**, *206*, 1−8. (c) Seiki, M. *Cancer Lett.* **2003**, *194*, 1−11.

(2) (a) Chakraborti, S.; Mandal, M.; Das, S.; Mandal, A.; Chakraborti, T. *Mol. Cell. Biol.* **2003**, *253*, 269−285. (b) Shiomi, T.; Lemaître, V.; D'Armiento, J.; Okada, Y. *Pathol. Int.* **2010**, *60*, 477−496. (c) Visse, R.; Nagase, H. *Circ. Res.* **2003**, *92*, 827−839. (d) Werb, Z.; Egeblad, M. *Nat. Rev.* **2002**, *2*, 161−174.

(3) Gialeli, C.; Theocharis, A. D.; Karamanos, N. K. *FEBS J.* **2011**, *278*, 16−27.

(4) Scherer, R. L.; McIntyre, J. O.; Matrisian, L. M. *Can. Met. Rev.* **2008**, *27*, 679−690.

(5) Weissleder, R. *Nat. Biotechnol.* **2001**, *19*, 316−317.

(6) Bremer, C.; Tung, C. H.; Weissleder, R. *Nat. Med.* **2001**, *7*, 743−748.

(7) Deguchi, J.; Aikawa, M.; Tung, C.; Aikawa, E.; Kim, D.; Ntziachristos, V.; Weissleder, R.; Libby, P. *Circulation* **2006**, *114*, 55−62.

(8) Yamane, T.; Hanaoka, K.; Muramatsu, Y.; Tamura, K.; Adachi, Y.; Miyashita, Y.; Hirata, Y.; Nagano, T. *Bioconjugate Chem.* **2011**, *22*, 2227−2236.

(9) (a) Aguilera, T. A.; Olson, E. S.; Timmers, M. M.; Jiang, T.; Tsien, R. T. *Integr. Biol.* **2009**, *1*, 371−381. (b) Olson, E. S.; Aguilera, R. A.; Jiang, T.; Ellies, L. G.; Nguyen, Q. T.; Wong, E. H.; Gross, L. A.; Tsien, R. Y. *Integr. Biol.* **2009**, *1*, 382−393.

(10) Jones, S. W.; Christison, R.; Bundell, K.; Voyce, C. J.; Brockbank, S. M. V.; Newham, P.; Lindsay, M. A. *Br. J. Pharmacol.* **2005**, *145*, 1093−1102.

(11) Kaplan, I. M.; Wadia, J. S.; Dowdy, S. F. *J. Controlled Release* **2005**, *102*, 247−253.

(12) Razkin, J.; Josserand, V.; Boturyn, D.; Jin, Z.; Dumy, P.; Favrot, M.; Coll, J.; Texier, I. *ChemMedChem* **2006**, *1*, 1069−1072.

(13) (a) Tung, C. H.; Lin, Y.; Moon, W. K.; Weissleder, R. *ChemBioChem* **2002**, *8*, 784−786. (b) Becker, A.; Hessenius, C.; Licha, K.; Ebert, B.; Sukowski, U.; Semmler, W.; Wiedenmann, B.; Grötzinger, C. *Nat. Biotechnol.* **2001**, *19*, 327−331. (c) Zheng, G.; Li, H.; Yang, K.; Blessington, D.; Licha, K.; Lund-Katz, S.; Chance, B.; Glickson, J. D. *Bioorg. Med. Chem. Lett.* **2002**, *12*, 1485−1488. (d) Chen, X. Y.; Conti, P. S.; Moats, R. A. *Cancer Res.* **2004**, *64*, 8009−8014. (e) Ke, S.; Wen, X. X.; Gurfinkel, M.; Charansangavej, C.; Wallace, S.; Sevick-Muraca, E. M.; Li, C. *Cancer Res.* **2003**, *63*, 7870−7875. (f) Ozmen, B.; Akkaya, E. U. *Tetrahedron Lett.* **2000**, *41*, 9185−9188. (g) Sasaki, E.; Kojima, H.; Nishimatsu, H.; Urano, Y.; Kikuchi, K.; Hirata, Y.; Nagano, T. *J. Am. Chem. Soc.* **2005**, *127*, 3684−3685. (h) Weissleder, R.; Tung, C.; Mahmood, U.; Bogdanov, A., Jr. *Nat. Biotechnol.* **1999**, *17*, 375−378. (i) Tung, C. H.; Bredow, S.; Mahmood, U.; Weissleder, R. *Bioconjugate Chem.* **1999**, *10*, 892−896.

(14) Loudet, A.; Burgess, K. *Chem. Rev.* **2007**, *107*, 4891−4932.

(15) (a) Koide, Y.; Urano, Y.; Hanaoka, K.; Terai, T.; Nagano, T. *ACS Chem. Biol.* **2011**, *6*, 600−608. (b) Fu, M.; Xiao, Y.; Qian, X.; Zhao, D.; Xu, Y. *Chem. Commun.* **2008**, *15*, 1780−1782.

(16) Jiang, T.; Olson, E. S.; Nguyen, Q. T.; Roy, M.; Jennings, P. A.; Tsien, R. Y. *Proc. Natl. Acad. Sci. U.S.A.* **2004**, *101*, 17867−17872.

(17) Johansson, M. K.; Cook, R. M. *Chem.— Eur. J.* **2003**, *9*, 3466−3471.

(18) Zhao, T.; Harada, H.; Teramura, Y.; Tanaka, S.; Itasaka, S.; Morinibu, A.; Shinomiya, K.; Zhu, Y.; Hanaoka, H.; Iwata, H.; Saji, H.; Hiraoka, M. *J. Controlled Release* **2010**, *144*, 109−114.

(19) (a) Komatsu, K.; Kikuchi, K.; Kojima, H.; Urano, Y.; Nagano, T. *J. Am. Chem. Soc.* **2005**, *127*, 10197−10204. (b) Cheng, D.; Shen, Q.; Nan, F.; Qian, Z.; Ye, Q. *Protein Expr. Purif.* **2003**, *27*, 63−74.

(20) Linder, K. E.; Metcalfe, E.; Nanjappan, P.; Arunachalam, T.; Ramos, K.; Skedzielewski, T. M.; Marinelli, E. R.; Tweedle, M. F.; Nunn, A. D.; Swenson, R. E. *Bioconjugate Chem.* **2011**, *22*, 1287−1297.